

Mismatch repair proteins expression and tumor-infiltrating T-cells in colorectal cancer

TAKAHIRO SHIGAKI¹, KENJI FUJIYOSHI¹, TOMOYA SUDO¹, AKIHIRO KAWAHARA²,
HIROYUKI NAKANE¹, TAKATO YOMODA¹, SACHIKO NAGASU¹, TETSUSHI KINUGASA¹,
JUN AKIBA², FUMIHIKO FUJITA¹ and YOSHITO AKAGI¹

Departments of ¹Surgery and ²Pathology, Kurume University School of Medicine, Kurume, Fukuoka 830-0011, Japan

Received January 26, 2022; Accepted May 31, 2022

DOI: 10.3892/ol.2022.13516

Abstract. Microsatellite instability (MSI) and tumor mutational burden (TMB) are indicators of the tumor mutational load, which can lead to immune cell recruitment. By contrast, the number of tumor-infiltrating T cells (TITs) is indicative of the host immune response to tumor cells. The present study evaluated if the expression of mismatch repair (MMR) proteins can be used as a precise tool to assess immunogenicity in the tumor microenvironment. A total of 73 colorectal cancer cases were enrolled in the present study. MMR protein expression was assessed using four-antibodies immunohistochemistry (IHC) targeting MLH1, MSH2, MSH6 and PMS2. TIT was assessed through IHC by counting CD3⁺ and CD8⁺ cells in tumor. The enrolled cases were classified into four groups according to MMR and TIT status i) Mismatch repair-proficient (pMMR) and a high number of TITs (pMMR/TIT-H); ii) pMMR and a low number of TITs (pMMR/TIT-L); iii) mismatch repair-deficient (dMMR) and TIT-H (dMMR/TIT-H); and iv) dMMR/TIT-L. The present study evaluated the clinicopathological characteristics of the four groups, in addition to the difference of TMB. TMB analysis was counted the number of the somatic mutations through multi-genes panel using next-generation sequencing. Clinicopathological characteristics, including age, sex, pathological depth of invasion

and lymph node metastasis, were not found to be statistically different between dMMR/TIT-H and dMMR/TIT-L groups. Tumors among pMMR/TIT-H group were associated with poorly differentiation compared with those in pMMR/TIT-L group (P=0.025). The median TMB among the dMMR/TIT-H group was the highest in four groups but the median TMB was <10 muts/Mb in dMMR/TIT-L, pMMR/TIT-H and pMMR/TIT-L groups, respectively. However, one tumor in the pMMR/TIT-H group showed high TMB. The present findings suggest that assessing MMR status alone may not be sufficient to precisely evaluate the antitumor immune response in the tumor microenvironment.

Introduction

Colorectal cancer (CRC) can be classified into mismatch repair-deficient (dMMR) and mismatch repair-proficient (pMMR) subtypes (1). dMMR CRC is characterized by a high tumor mutational burden (TMB) and high infiltration rates of activated CD8⁺ cytotoxic T lymphocytes (CTLs) (2). These features contribute to the generally superior therapeutic outcomes of immunotherapy, including immune checkpoint inhibitors (ICIs), in patients with dMMR CRC (3). Compared with dMMR CRC, pMMR CRC exhibits a low TMB and few tumor-infiltrating lymphocytes, leading to immune tolerance and evasion in the tumor microenvironment (4). However, previous studies have shown that immune cell infiltration can be used for the subtype classification of CRC regardless of MMR protein expression (5,6), since a fraction of pMMR CRCs are also relatively immunogenic (2). As pMMR CRCs with high TMB can potentially respond to ICIs (7), it is reasonable to assess the immune response status based on MMR protein expression in combination with other biomarkers capable of evaluating immune reactions in the tumor microenvironment, such as a scoring system from immunohistochemistry (8).

Although the methods used for assessing MMR protein expression, TMB and for determining the number of tumor-infiltrating T cells (TITs) are similar, each one focuses on a different aspect of tumor biology. MMR protein expression analysis and TMB tests can be used to indicate the tumor mutation load, which can lead to immune cell recruitment (9). By contrast, TITs are indicative of the host immune response to the tumor (10). Therefore, the present study evaluated whether

Correspondence to: Dr Kenji Fujiyoshi, Department of Surgery, Kurume University School of Medicine, 67 Asahi-machi, Kurume, Fukuoka 830-0011, Japan
E-mail: fujiyoshi_kenji@med.kurume-u.ac.jp

Abbreviations: CRC, colorectal cancer; CT, center of the tumor; dMMR, mismatch repair-deficient; FFPE, formalin-fixed, paraffin-embedded; ICI, immune checkpoint inhibitor; IM, invasive margin; MDSC, myeloid-derived suppressor cell; Mb, megabases; M2M, M2 macrophage; MMR, mismatch repair; MSI, microsatellite instability; NGS, next-generation sequencing; pMMR, mismatch repair-proficient; TIT, tumor-infiltrating T cell; TMB, tumor mutational burden; UICC, Union for International Cancer Control

Key words: colorectal carcinoma, clinical outcome, antitumor immunity, cancer immunotherapy

MMR protein expression alone is a viable and precise tool for assessing immunogenicity in the tumor microenvironment when combined with TIT analysis and TMB testing.

Materials and methods

Patients and samples. All 73 patients (mean age, 71.4±10.4 years; female, n=33; male, n=40) enrolled into this study were diagnosed with CRC and underwent surgical treatment at the Kurume University Hospital (Kurume, Japan) between January and December 2017. All of the resected tumor samples were immersed in a solution of 10% neutral-buffered formalin for about 18–24 h at room temperature and were collected, dehydrated with ethanol, infiltrated with paraffin wax, embedded into paraffin at 60°C and then cooled to become formalin fixed, paraffin embedded (FFPE) tissue blocks. Patients who underwent preoperative chemotherapy/chemoradiotherapy or had multiple cancers were excluded. Clinical data, including age, sex and anatomical tumor location, were obtained from the Kurume University Hospital pathology databases. Postoperative pathological staging of the resected specimens was conducted according to the seventh edition of the Tumor, Node, and Metastasis classification scheme of the Union for International Cancer Control (UICC) (11). The surgeons involved in the study reviewed patient medical records for information regarding their clinical outcomes and pathology records. Informed consent was obtained from all 73 patients enrolled in the present study, which was conducted in accordance with the provisions of The Declaration of Helsinki and approved by the institutional ethical review board of Kurume University Hospital (approval no. 388).

Analysis of MMR protein expression. MMR protein expression was assessed using a four-antibody immunohistochemical assay targeting MutL homolog 1 (MLH1 clone; ES05; cat. no. M3640), MutS homolog 2 (MSH2 clone; FE11; cat. no. 556349), MutS homolog 6 (MSH6 clone; EP49; cat. no. 287R) and post-meiotic segregation 1 homolog 2 (PMS2 clone; EP51; cat. no. M3647) and the DAKO EnVision system (Dako; Agilent Technologies, Inc.), as previously described (12). The Autostainer Link 48 and PT link (Agilent Technologies, Inc.) were used for automated immunostaining system. Tissue sections (4-μm-thick) were deparaffinized and pretreated with heat-induced epitope retrieval at 97°C for 20 min at high pH (Target retrieval solution; diluted 1:50; cat. no. K8023) using PT link (Agilent Technologies, Inc.). The slides were then incubated with blocking reagent (Peroxidase-blocking reagent; ready to use; cat. no. SM801) for 5 min at room temperature. The slides were then incubated with the following antibodies: MLH1, MSH2, MSH6 and PMS2, for 30 min at room temperature, and incubated with secondary antibody (EnvisionFLEX+ LINKER kit; ready to use; cat. no. K8021; Agilent Technologies, Inc.) for 30 min at room temperature using Autostainer Link 48. After washing in Tris-buffered saline, the slides were visualized using 3, 3'-diaminobenzidine (DAB) as the nuclear stain. All IHC results were evaluated using a light microscope. Loss of MMR proteins expression was defined as the absence of nuclear expression in tumor cells in five fields of view compared with positive nuclear expression in corresponding normal epithelial

cells. Patients showing loss of expression for ≥ one of MMR proteins in the tumor epithelium would be diagnosed as CRC with dysfunctional MMR (dMMR CRC).

Analysis of T-cell densities. FFPE tissue sections (4-μm thick) were prepared and placed on coated glass slides. The tissue sections were labeled with antibodies using the fully automated Bond-III autostainer (Leica Microsystems, Ltd.) as previously described (12). Primary antibodies against CD3⁺ (clone LN10; diluted 1:300; cat. no. NCL-L-CD3-565; Leica Microsystems, Ltd.) and CD8⁺ (clone 4B11; diluted 1:200; cat. no. NCL-L-CD8-4B11; Leica Microsystems, Ltd.) were used for immunostaining. Tissue sections were deparaffinized using dewax solution (ready to use; cat. no. AR9222; Leica Microsystems, Ltd.), and the slides were then incubated with blocking reagent (peroxidase-blocking reagent; 3–4% hydrogen peroxide solution), including a Refine polymer detection system (ready to use; cat. no. DS9800; Leica Microsystems, Ltd.) for 5 min at room temperature (~25°C). CD3⁺ and CD8⁺ antibodies were heat-treated using epitope retrieval solution 2 (pH 9.0) for 20 min at 99°C, and incubated with CD3⁺ and CD8⁺ as primary antibodies for 15 min at room temperature (~25°C). This automated system used a Refine polymer detection system with HRP (Horseradish peroxidase)-polymer as secondary antibody and DAB as the nuclear stain, and incubated with secondary antibody for 8 min at room temperature (~25°C). The slides were visualized using DAB. Fig. S1 shows representative images of immunohistochemical staining of CD3⁺ and CD8⁺ in the center of the tumor (CT) and the invasive margin (IM).

All stained slides were scanned and digitized using a NanoZoomer 2.0-HT: C9600-13 slide scanner (Hamamatsu Photonics KK). The scanned images were analyzed using the NDP.view2 viewing software (Hamamatsu Photonics KK). In total, five areas in each of the CT and the IM were captured (magnification, x200) and stored as JPEG images. The captured images were processed using the ImageJ software (version 1.50i) (13) to quantify CD3⁺ and CD8⁺ cells in the tissue specimens, as previously described (12). HUGO Gene Nomenclature Committee-approved symbols and root symbols are used for genes and gene families, including *BRCA*, *CD3*, *CD8*, *MLH1*, *MSH2*, *MSH6*, *PDCD1*, *PMS2*, *POLD*, *POLD1*, *POLD2*, *POLE* and *RAD*; all of which are described at www.genenames.org. Italicized gene symbols indicate gene names and non-italicized gene symbols indicate gene product names (14).

Evaluation of the number of TITs. After the quantified values of numbers of CD3⁺ and CD8⁺ cells in CT and IM were obtained, the median values of each marker in CT and IM were calculated. According to each CD3⁺ and CD8⁺ median value, following high-CD3⁺, low-CD3⁺, high-CD8⁺ and low-CD8⁺ in each CT and IM could be determined. Low-CD3⁺ or low-CD8⁺ was 0 points and 1 point was given to high-CD3⁺ or high-CD8⁺ in each CT and IM. TIT score (from I0 to I4) was acquired from the total points of CT and IM that were determined with each CD3 and CD8 status (8,12,15).

Analysis of TMB. DNA was extracted from specimens that had been cryopreserved following excision using the AllPrep

DNA/RNA/Protein Mini kit (Qiagen GmbH) according to the manufacturer's protocols. TMB analysis was performed using the OncoPrint™ Tumor Mutation Load Assay (cat. no. A37909; Thermo Fisher Scientific, Inc.), which is a PCR-based next-generation sequencing (NGS) assay. For each sample's quality test, TM Qubit M dsDNA BR Assay kit (Thermo Fisher Scientific) was utilized. TaqMan M Universal PCR Master Mix (Thermo Fisher Scientific) and TaqMan M RNase P Detection Reagents (Thermo Fisher Scientific) were used to confirm amplification and fragmentation by quantitative qPCR. Each sample was confirmed to have a Qubit quantitative concentration/qPCR quantitative concentration value ≥ 0.5 .

Library preparation required 200 ng input DNA extracted from frozen specimens. This multi-gene target sequencing panel covers 1.7 megabases (Mb) of 409 genes, which are known to be associated with cancer development, including 1.2 Mb exonic and 0.45 Mb intronic regions. The panel consists of 15,513 PCR targets that are evenly distributed in two pools. The Agilent SureSelect Human All Exon V5 kit (Agilent Technologies, Inc.; with 50 Mb panel) was used for target capture from 200 ng input DNA followed by sequencing on HiSeqX (Illumina, Inc.). All single base substitutions with allele frequency $\geq 5\%$ were considered. TMB was defined as the number of nonsynonymous somatic mutations per Mb (mut/Mb), including missense and nonsense point mutations, in the exonic genome regions examined. Germline variants were removed using a germline filter chain based on information in population databases (1000 Genome Project (<https://www.internationalgenome.org/>), NHLBI GO Exome Sequencing Project (<https://esp.gs.washington.edu/drupal/>), and ExAC; <https://gnomad.broadinstitute.org/>). After computational germline mutation filtering, reads were aligned to hg19 using Torrent Suite 5.8 and BAM files were transferred to Ion Reporter 5.1 for variant calling and secondary analysis, including TMB calculation, which is an analysis workflow optimized mapping and variant calling parameters. This method was previously validated for accuracy in whole-exome sequencing (16). Patients with available TMB data were divided into two groups. Those with TMB ≥ 10 mut/Mb were classified into the TMB-H group, whereas those with TMB < 10 mut/Mb were classified in the TMB-L group (17).

TMB analysis was performed on the 12 of the 73 cases which had sufficient frozen tumor tissue. TMB analysis was performed for 12 cases in total, including three dMMR cases with a high number of TITs (dMMR/TIT-H), two dMMR cases with a low number of TITs (dMMR/TIT-L), four pMMR cases with TIT-H (pMMR/TIT-H) and three pMMR cases with TIT-L (pMMR/TIT-L).

Statistical analysis. All statistical analyses were conducted using the JMP software (version 13.0; SAS Institute, Inc.). P-values were determined using two-sided tests, with a two-sided α level of 0.05 used as the threshold for statistical significance. Age was analyzed with the Wilcoxon rank sum test. The χ^2 test was used to evaluate association among MMR protein expression, the number of TITs and clinicopathological characteristics. Fisher's exact test was used for the analysis of characteristics between dMMR and pMMR in Table I, the analysis of associations between MMR protein expression and the number of TITs in Table II, and the analysis of characteristics for TIT-H and TIT-L

in Table III. Spearman's correlation analysis was used to analyze correlations between TMB and T-cell densities.

Results

Characteristics of patients with CRC according to their MMR protein expression and the number of TITs. The present study investigated 73 patients with CRC and available clinicopathological data, including MMR protein expression and the number of TITs. In total, 10/73 patients (13.7%) were diagnosed with dMMR CRC, whereas 32/73 patients (43.8%) were assessed as having CRC with TIT-H. Table I summarizes the clinical, pathological and molecular characteristics according to MMR protein expression and the number of TITs. dMMR was positively associated with female sex ($P=0.04$), a proximal-sided tumor location ($P=0.006$) and histologically poor differentiation ($P=0.01$). TIT-H was positively associated with histologically poor differentiation ($P=0.02$) and inversely associated with an advanced disease stage according to the UICC staging system ($P=0.04$).

Association between MMR protein expression and the number of TITs. Table II and Fig. S2 show the association between MMR protein expression and the number of TITs. Although the frequency of TIT-H was higher in the dMMR group (60%) compared with that in the pMMR group (41.2%), 40% of the patients in the dMMR group were TIT-L. However, the association between MMR protein expression and the number of TITs was not statistically significant ($P=0.32$).

Table III shows that the clinicopathological characteristics tested, namely age, sex, pathological depth of invasion and lymph node metastasis, were not statistically different between the dMMR/TIT-H and dMMR/TIT-L groups. In the pMMR group, pMMR/TIT-H was associated with poor differentiation compared with pMMR/TIT-L ($P=0.025$; Table III).

Analysis of association of TMB with MMR protein expression and the number of TITs. Among the 73 patients, tumor tissues were available from 12 patients (Table SI). Therefore, their tumor DNA was subjected to NGS analysis to obtain the TMB data. The associations of TMB with MMR protein expression and the number of TITs were subsequently analyzed (Table IV). TMB ranged from 2.51 to 54.7 mut/Mb in all samples. Among the four designated groups, the median TMB reached the highest value in the dMMR/TIT-H group but was below < 10 mut/Mb in the dMMR/TIT-L, pMMR/TIT-H and pMMR/TIT-L groups. All cases in the dMMR/TIT-H group were TMB-H, whereas all the cases in the dMMR/TIT-L group were TMB-L. pMMR was associated with TMB-L regardless of the TIT number, although one case in the pMMR/TIT-H group (case ID 6) showed TMB-H. The MMR protein expression and the number of TITs in the 12 cases were ranked according to TMB (Fig. 1). Regarding MMR protein expression, two cases (case IDs 4 and 5), which showed both TIT-L and TMB-L in the dMMR group, showed isolated loss of PMS2 expression (Fig. 1). Among the dMMR cases, three cases with both TIT-H and TMB-H were found. In particular, both MLH1 and PMS2 expression were lost in three cases (case IDs 1, 2 and 3; Fig. S3). Correlation analysis of TMB and TITs revealed that TMB was associated with the densities of CD3⁺ and CD8⁺ in the CT (CD3⁺, $r=0.76$ and

Table I. Characteristics of patients with colorectal cancer according to their MMR protein expression and the number of TITs.

Characteristics ^a	Total (n=73)	MMR-protein expression		P-values	Number of TITs		P-values
		MMR- proficient (n=63)	MMR- deficient (n=10)		TIT-low (n=41)	TIT-high (n=32)	
Sex				0.036 ^b			0.46 ^c
Male	40 (54.8%)	38 (60.3%)	2 (20.0%)		24 (58.8%)	16 (50.0%)	
Female	33 (45.2%)	25 (39.7%)	8 (80.0%)		17 (41.2%)	16 (50.0%)	
Mean \pm SD age, years		70.9 \pm 10.1	74.7 \pm 12.4	0.32 ^d	70.4 \pm 10.6	72.6 \pm 10.3	0.42 ^d
Tumor location				0.006 ^b			0.085 ^c
Distal (descending colon to rectum)	51 (69.9%)	48 (76.2%)	3 (30.0%)		32 (78.1%)	19 (59.4%)	
Proximal (cecum to splenic flexure)	22 (30.1%)	15 (23.8%)	7 (70.0%)		9 (21.9%)	13 (40.6%)	
pT stage (depth of tumor invasion)				0.71 ^b			0.38 ^c
T1-2 (submucosa or muscularis propria)	21 (29.2%)	19 (30.6%)	2 (20.0%)		10 (25.0%)	11 (34.4%)	
T3-4 (subserosa or serosa or other organs)	51 (70.8%)	43 (69.4%)	8 (80.0%)		30 (75.0%)	21 (65.6%)	
pN stage (number of positive lymph nodes)				0.74 ^b			0.11 ^c
N0 (0)	38 (52.1%)	32 (50.8%)	6 (60.0%)		18 (43.9%)	20 (62.5%)	
N1-3 (\geq 1)	35 (47.9%)	31 (49.2%)	4 (40.0%)		23 (56.1%)	12 (37.5%)	
Union for International Cancer Control disease stage				0.62 ^c			0.04 ^c
Stage I	15 (20.5%)	13 (20.6%)	2 (20.0%)		7 (17.1%)	8 (25.0%)	
Stage II	20 (27.4%)	16 (25.4%)	4 (40.0%)		8 (19.5%)	12 (37.5%)	
Stage III	27 (37.0%)	25 (39.7%)	2 (20.0%)		16 (39.0%)	11 (34.4%)	
Stage IV	11 (15.1%)	9 (14.3%)	2 (20.0%)		10 (24.4%)	1 (3.1%)	
Tumor differentiation				0.01 ^b			0.008 ^c
Well-moderate	65 (89.0%)	59 (93.7%)	6 (60.0%)		40 (97.6%)	25 (78.2%)	
Poor	8 (11.0%)	4 (6.3%)	4 (40.0%)		1 (2.4%)	7 (21.8%)	
Lymphatic invasion				1.0 ^b			0.54 ^c
Negative	45 (61.6%)	39 (61.9%)	6 (60.0%)		24 (58.5%)	21 (65.6%)	
Positive	28 (38.4%)	24 (38.1%)	4 (40.0%)		17 (41.5%)	11 (34.4%)	
Venous invasion				0.71 ^b			0.23 ^c
Negative	22 (30.1%)	20 (31.7%)	2 (20.0%)		10 (24.4%)	12 (37.5%)	
Positive	51 (69.9%)	43 (68.3%)	8 (80.0%)		31 (75.6%)	20 (62.5%)	

^aData presented as N (%) patients with a specific clinical, pathological or molecular characteristic among all patients apart from age, which was presented as the mean \pm SD. ^bFisher's exact test was conducted to analyze associations among MMR protein expression and clinicopathological characteristics. ^c χ^2 tests were conducted to analyze associations among the number of TITs and clinicopathological characteristics. ^dAge was analyzed with the Wilcoxon rank sum test. MMR, mismatch repair; TITs, tumor-infiltrating T lymphocytes; SD, standard deviation.

P=0.004; CD8⁺, r=0.76 and P=0.004), but not in the IM (CD3⁺, r=0.35 and P=0.25; CD8⁺, r=0.35 and P=0.26; Table V; Fig. S4).

Discussion

The present study evaluated if MMR protein expression alone could be a viable measure to assess immunogenicity in the tumor microenvironment, using TIT analyses and TMB tests. The frequency of TIT-H was higher in the dMMR group compared with that in the pMMR group, but 40% of dMMR

cases were TIT-L. Among the dMMR cases, three cases with dMMR/TIT-H were TMB-H, whereas the dMMR/TIT-L group was TMB-L. pMMR was found to be associated with TMB-L regardless of the number of TITs, although one case in the pMMR/TIT-H group (case ID 6) showed TMB-H. In total, two cases in the dMMR group showed both TIT-L and TMB-L cases and isolated loss of PMS2 expression (case IDs 4 and 5). These findings suggest that MMR protein expression alone is a rather imprecise measure for assessing tumor immunogenicity and antitumor immunity in the tumor microenvironment.

Table II. Association between MMR protein expression and the number of TITs.

Number of TITs	MMR proteins expression ^a		P-value ^b
	MMR-proficient (n=63) (%)	MMR-deficient (n=10) (%)	
Low (n=41)	37 (58.7)	4 (40.0)	0.32
High (n=32)	26 (41.2)	6 (60.0)	

^aData presented as the N (%) of patients with the indicated MMR protein expression status and the number of TITs. ^bFisher's exact test was used to analyze associations between MMR protein expression and the number of TITs. MMR, mismatch repair; TITs, tumor-infiltrating T cells; TIT-H, high number of tumor-infiltrating T cells; TIT-L, low number of tumor-infiltrating T cells.

Table III. Characteristics of patients with colorectal cancer according to MMR protein expression and the number of TITs.

Characteristics ^a	MMR-proficient		P-value	MMR-deficient		P-value
	TIT-low (n=37)	TIT-high (n=26)		TIT-low (n=4)	TIT-high (n=6)	
Sex			0.72 ^b			1.0 ^c
Male	23 (62.2%)	15 (57.7%)		1 (25.0%)	1 (16.7%)	
Female	14 (37.8%)	11 (42.3%)		3 (75.0%)	5 (83.3%)	
Mean ± SD age, years	70.4±10.5	71.5±9.7	0.34 ^d	70.5±12.8	77.5±12.5	0.34 ^d
Tumor location			0.28 ^b			0.5 ^c
Distal (descending colon to rectum)	30 (81.1%)	18 (69.2%)		2 (50.0%)	1 (16.7%)	
Proximal (cecum to splenic flexure)	7 (18.9%)	8 (30.8%)		2 (50.0%)	5 (83.3%)	
pT stage (depth of tumor invasion)			0.56 ^b			0.47 ^c
T1-2 (submucosa or muscularis propria)	10 (27.8%)	9 (34.6%)		0 (0%)	2 (33.3%)	
T3-4 (subserosa or serosa or other organs)	26 (72.2%)	17 (65.4%)		4 (100%)	4 (66.7%)	
pN stage (number of positive lymph nodes)			0.35 ^b			0.19 ^c
N0 (0)	17 (45.9%)	15 (57.7%)		1 (25.0%)	5 (83.3%)	
N1-3 (≥1)	20 (54.1%)	11 (42.3%)		3 (75.0%)	1 (16.7%)	
Union for International Cancer			0.17 ^b			0.18 ^b
Control disease stage						
Stage I	7 (18.9%)	6 (23.1%)		0 (0%)	2 (33.3%)	
Stage II	7 (18.9%)	9 (34.6%)		1 (25.0%)	3 (50.0%)	
Stage III	15 (40.6%)	10 (38.4%)		1 (25.0%)	1 (16.7%)	
Stage IV	8 (21.6%)	1 (3.9%)		2 (50.0%)	0 (0%)	
Tumor differentiation			0.025 ^c			0.57 ^c
Well-moderate	37 (100%)	22 (84.6%)		3 (75.0%)	3 (50.0%)	
Poor	0 (0%)	4 (15.4%)		1 (25.0%)	3 (50.0%)	
Lymphatic invasion			0.63 ^b			1.0 ^c
Negative	22 (59.5%)	17 (65.4%)		2 (50.0%)	4 (66.7%)	
Positive	15 (40.5%)	9 (34.6%)		2 (50.0%)	2 (33.3%)	
Venous invasion			0.34 ^b			0.47 ^c
Negative	10 (27.0%)	10 (38.5%)		0 (0%)	2 (33.3%)	
Positive	27 (73.0%)	16 (61.5%)		4 (100.0%)	4 (66.7%)	

^aData are presented as N (%), representing the proportions of patients with specific clinical, pathological or molecular characteristics. ^bχ² tests were conducted to analyze associations between MMR-proficient and the number of TITs. ^cFisher's exact test was conducted to analyze associations between MMR-deficient and the number of TITs. ^dAge was analyzed with the Wilcoxon rank sum test. MMR, mismatch repair; TITs, tumor-infiltrating T cells; SD, standard deviation.

Table IV. Associations of TMB with MMR proteins expressions and the number of TITs.

Parameter	MMR-proficient		MMR-deficient	
	TIT-low (n=3)	TIT-high (n=4)	TIT-low (n=2)	TIT-high (n=3)
TMB ^a	4.2 (3.35-5.84)	3.35 (2.5-42.1)	9.2 (9.18-9.22)	22.5 (16.7-26.3)
TMB-low (n=8) ^b	3	3	2	0
TMB-high (n=4) ^b	0	1	0	3

^aData are presented as median (interquartile range). ^bData are presented as N. MMR, mismatch repair; TMB, tumor mutational burden; TIT, tumor-infiltrating T cell.

Table V. Correlations between TMB and number of TITs.

Type of TITs	TMB	
	p(95% CI)	P-value ^a
CD3 ⁺		
CT (n=12)	0.76 (0.33-0.93)	0.036
IM (n=12)	0.36 (-0.27-0.77)	0.66
CD8 ⁺		
CT (n=12)	0.76 (0.33-0.93)	0.027
IM (n=12)	0.35 (-0.28-0.77)	0.47

^aCorrelation coefficients between the TMB and number of TITs and P-values were calculated using Spearman's rank correlation coefficient analysis. TIT, tumor-infiltrating T cell; TMB, tumor mutational burden; r, correlation coefficient; CT, center of the tumor; IM, invasive margin.

Consideration of parameters other than MMR protein expression, such as the number of TITs and TMB, may strengthen the assessment of tumor immunogenicity for screening patients who may benefit from ICI therapy.

dMMR CRCs are caused by MMR dysfunction, which can result in increased TMB and the generation of neoantigens, which are antigens resulting from the tumor somatic mutations that confer tumor immunogenicity and can elicit an antitumor immune response (9). T cells activated in response to abundant neoantigens in the tumor microenvironment can suppress tumor proliferation and progression (4). Therefore, ICIs have exerted effective responses among dMMR CRCs because of the high immunogenicity in the tumor microenvironment (3,18). A large-scale case study previously reported microsatellite instability (MSI)-high (MSI-H) and immunoscore-low cases in 2.7% (15/550) of all CRC cases tested (19), suggesting that a fraction of the patients with MSI-H CRC showing low immune reaction might show relatively low TMB levels. MMR dysfunction results from a loss of function in any of the MMR genes encoding the four MMR proteins, MLH1, MSH2, MSH6 and PMS2. Because MLH1 and MSH2 are essential for MMR function, their deficiency causes a large decrease in MMR function (20). While *MLH1* mutation represents loss of both MLH1 and PMS2 protein expression, *PMS2* mutation represents isolated loss of PMS2 protein expression not

loss of MLH1 protein expression. MLH1 and PMS2 proteins form a heterodimer, MLH1 protein is a key function of MMR compared to PMS2 protein. Therefore, isolated PMS2 loss of expression are due to *PMS2* mutation, not *MLH1* mutation (21). Moreover, Lynch syndrome patients harboring *PMS2* germline mutation is lower risk of colorectal cancer incidence (22), which may explain why the isolated loss of PMS2 results in milder forms of MMR dysfunction and lower TMB levels (22,23). Therefore, CRC with isolated loss of PMS2 expression can show reduced TMB levels (22). In the present study, three out of the five cases in the dMMR group had both high TMB levels and TIT-H who also showed the loss of either MLH1 or MSH2 expression, whereas the other two showed dMMR/TIT-L with the isolated loss of PMS2 expression. Although the number of insertion/deletion variants tend to be more strongly correlated with tumor-infiltrating lymphocyte (TIL) densities compared with TMB (24), the MMR protein expression status and the number of TIT were not found to be significantly associated with the number of insertion/deletion variants in this study. Given the association between MMR protein function and TMB levels (24,25), CRCs with isolated loss of PMS2 expression show lower levels of TMB and immune cell infiltration compared with those with MLH1 and MSH2 expression (26). Accordingly, the present findings indicated that CRCs with isolated loss of PMS2 expression showed a lower TMB level and number of TITs showed loss of both MLH1 and PMS2. This suggests that an MMR protein expression assay considering the patterns of MMR protein expression (isolated loss of PMS2 vs. loss of both MLH1 and PMS2) may provide an improved estimation of the degree of immunogenicity compared with that of the MSI analysis.

In a number of studies on the ICI treatment of CRCs with MSI, 85% of CRCs with MSI and low TMB failed to respond to immune checkpoint blockade (4,28). In CRCs with microsatellite stability (MSS), TMB-L and a lack of immune cell infiltration have been posited as mechanisms underlying immune resistance (5,27). CRCs with MSS have a low mutation load in tumor cells (29,30) and a low number of presenting antigens, leading to a lower level of T-cell infiltration in the tumor microenvironment (4). However, previous studies have reported that 21-50% of CRCs with MSS actually showed high T-cell infiltration (19,31,32). In addition, pMMR CRCs with a high number of TILs showed therapeutic response to ICIs (30,33), suggesting that pMMR CRCs harbor antitumor immunogenic potential and may be therapeutically responsive to ICIs. Although MMR protein

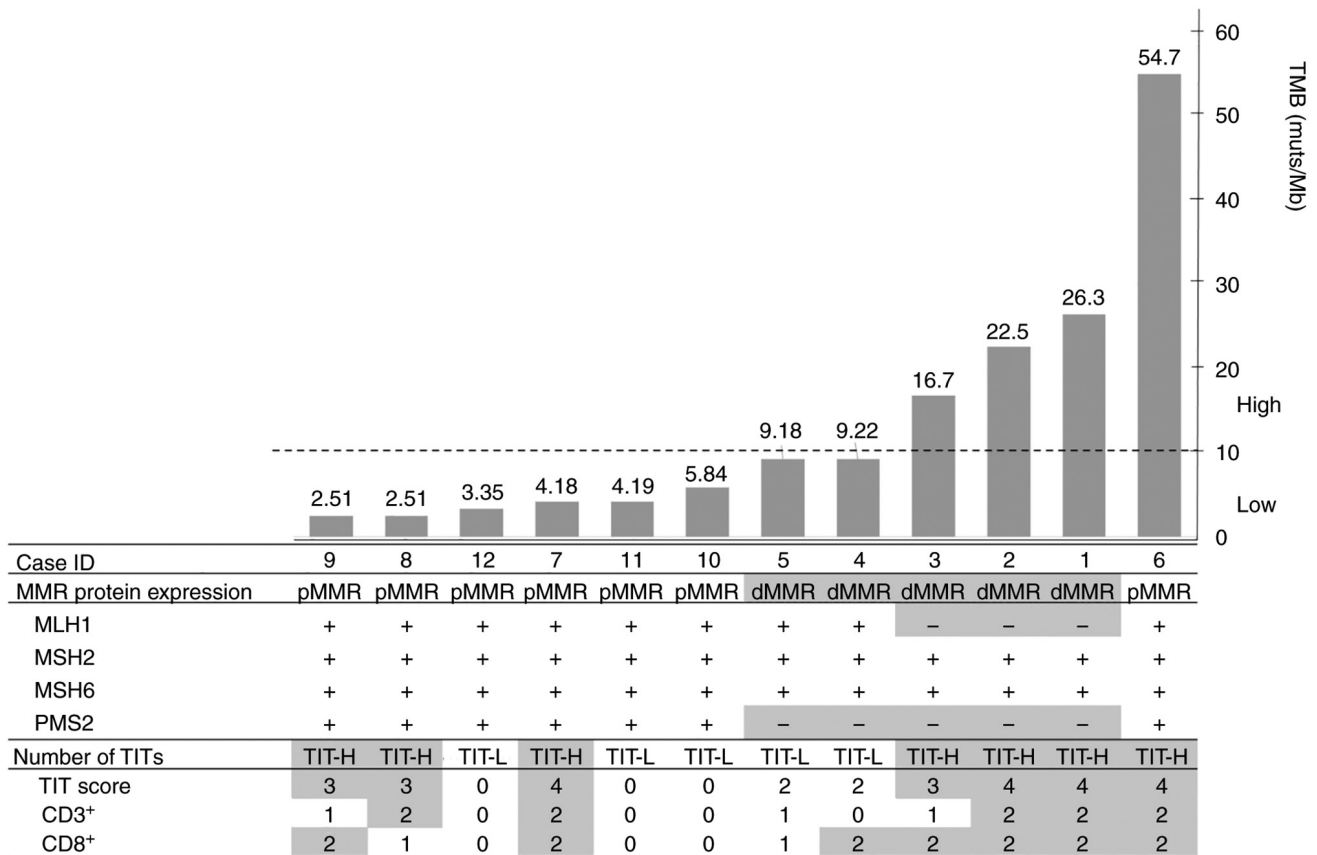


Figure 1. Association analysis of TMB with MMR protein expression and the number of TITs. Colorectal cancer cases were arranged according to TMB levels, the MMR protein expression status and the number of TITs. The cases were additionally divided into two groups based on the TMB level, as shown by the dotted line. The sections highlighted in gray represent dMMR, loss of MMR protein expression, TIT-H and the high numbers of CD3⁺ and CD8⁺ cells in the figure. TMB-L, TMB <10; TMB-H, TMB ≥10. MMR, mismatch repair; MLH1, MutL homolog 1; MSH, MutS homolog; PMS2, post-meiotic segregation 1 homolog 2; dMMR, mismatch repair-deficient; pMMR, mismatch repair-proficient; TMB, tumor mutational burden; TIT-H, high number of tumor-infiltrating T cells; TIT-L, low number of tumor-infiltrating T cells; muts/Mb, mutations per megabases.

expression can predict immunogenicity, it cannot reflect the number of TITs. Compared with MMR protein expression, the number of TITs, such as Immunoscore (a scoring tool used to assess the immune response by counting the densities of infiltrating CD3⁺ and CD8⁺ T cells at the CT and IM of colorectal tumors) (31), can serve as a biomarker for assessing not only immunogenicity, but also responsiveness to ICIs (34). In line with findings in previous studies, among the seven cases in the pMMR group, three cases showed both TIT-L and TMB-L, whereas the remaining four cases showed TIT-H. These four cases showing both pMMR and TIT-H may have activated antitumor immunity. Therefore, considering not only MMR proteins expression, but also additional parameters, such as the number of TITs and TMB level, may strengthen the tumor immunogenicity assessment.

The present study had several limitations. Due to the limited number of CRC tissue samples, only MMR function among the DNA-repair mechanisms was evaluated, without considering base-excision repair, nucleotide-excision repair or homologous recombination (35). Several of the pMMR CRCs are highly immunogenic owing to dysfunction in the DNA-repair-related proteins other than those involved in MMR, including ataxia telangiectasia mutated kinase, ataxia telangiectasia and Rad3 related kinase, BRCA, DNA polymerase ϵ (*POLE*), DNA polymerase δ 1 (*POLD1*), DNA

polymerase δ 2 (*POLD2*) and *RAD* (36). Although these CRCs are generally not of the MSI-H/dMMR subtype, they can also be highly immunogenic (29,30). In a large CRC cohort study, 3% of MSS tumors were previously identified to be TMB-H, which harbored somatic *POLE*, *MSH6* and *MSH2* mutations (37). Additionally, MSS tumors with *POLE* mutation have demonstrated promising clinical responses to the anti-PDCD1(PD-1) ICI, nivolumab (38). In the present study, one out of the seven cases of pMMR CRCs were TMB-H. Therefore, this CRC may harbor a *POLE* or *POLD1* mutation, although any potential mutations in these genes were not analyzed. In pMMR CRCs, DNA-repair dysfunctions other than those associated with MMR genes can increase immunogenicity, leading to TIT-H (30). Therefore, assessing other DNA-repair genes, as well as MMR genes according to MMR protein expression, may be useful for designing and monitoring ICI treatment regimens. CD3⁺ and CD8⁺ were examined to accurately evaluate immunogenicity in the present study. However, the presence of immunosuppressive cells, such as M2 macrophages (M2Ms) and myeloid-derived suppressor cells (MDSCs), were not examined in the microenvironment. M2Ms and MDSCs can suppress T-cell infiltration, leading to immunosuppression (39). In addition, a previous study reported that pMMR CRCs showed high levels of M2Ms and MDSCs in the tumor

microenvironment (4). Therefore, accurate evaluation of the tumor immune status, including M2M and MDSC levels, is warranted in future studies. Based on the present findings, it cannot conclude that ICI treatment would be effective for patients with pMMR/TIT-H CRC because ICI treatment was not given to the patients enrolled in the present study. Furthermore, a clinical trial was not performed to determine if the combined analysis of MMR protein expression and the number of TITs would improve the accuracy in estimating the ICI response. However, the present study provides preliminary data for designing future clinical trials. The present study was a single-center retrospective study with a small cohort size. In addition, TMB could not be examined in all cases, since the relevant data were available in only 12 cases. Therefore, the statistical power of the present study was limited, where larger sample sizes are required to strengthen the findings. However, the results were similar to those of large-scale trials (40,41), supporting the accuracy of the findings.

In conclusion, determining MMR proteins expression alone may not be a sufficiently precise assay for tumor immunogenicity and antitumor immunity in the tumor microenvironment of CRC tumors. Furthermore, the present study suggests that considering not only MMR proteins expression, but also other parameters, such as the number of TITs and TMB, may strengthen the assessment of tumor immunogenicity for the screening of patients who may benefit from ICI therapy.

Acknowledgements

Not applicable.

Funding

The present study was supported by the Kurume University Research Branding Project.

Availability of data and materials

The datasets used and/or analyzed during the current study are available from the corresponding author on reasonable request. The datasets generated during and/or analyzed during the current study are available in the PSUB017737 repository, <https://ddbj.nig.ac.jp/DRASearch/>.

Authors' contributions

KF, TSu and TSh took part in conceptualization and methodology. HN, SN, TSh performed the experiments. FF, HN, TY, SN, TK and YA obtained and handled colorectal specimens and clinical data. AK and JA performed the histological examination of the samples and clinical data. AK, KF, TSu and TSh analyzed the data and were major contributors in writing the manuscript. FF, JA, TK and YA confirm the authenticity of all the raw data. HN, TY, SN and AK organized the tables. KF, TSh and TSu were involved in the preparation of the figure. TK, FF and YA reviewed and edited the article. All authors read and approved the final manuscript.

Ethics approval and consent to participate

The present study was conducted in accordance with the provisions of The Declaration of Helsinki and approved by the institutional ethical review board of Kurume University Hospital (approval no. 388; Kurume, Japan). Informed consent was obtained from all 73 patients enrolled in the study.

Patient consent for publication

Not applicable.

Competing interests

The authors declare that they have no competing interests.

References

1. Llosa NJ, Cruise M, Tam A, Wicks EC, Hechenbleikner EM, Taube JM, Blosser RL, Fan H, Wang H, Luber BS, *et al*: The vigorous immune microenvironment of microsatellite instable colon cancer is balanced by multiple counter-inhibitory checkpoints. *Cancer Discov* 5: 43-51, 2015.
2. Ganesh K, Stadler ZK, Cercek A, Mendelsohn RB, Shia J, Segal NH and Diaz LA Jr: Immunotherapy in colorectal cancer: Rationale, challenges and potential. *Nat Rev Gastroenterol Hepatol* 16: 361-375, 2019.
3. Le DT, Uram JN, Wang H, Bartlett BR, Kemberling H, Eyring AD, Skora AD, Luber BS, Azad NS, Laheru D, *et al*: PD-1 blockade in tumors with mismatch-repair deficiency. *N Engl J Med* 372: 2509-2520, 2015.
4. Picard E, Verschoor CP, Ma GW and Pawelec G: Relationships between immune landscapes, genetic subtypes and responses to immunotherapy in colorectal cancer. *Front Immunol* 11: 369, 2020.
5. Galon J, Costes A, Sanchez-Cabo F, Kirilovsky A, Mlecnik B, Lagorce-Pagès C, Tosolini M, Camus M, Berger A, Wind P, *et al*: Type, density, and location of immune cells within human colorectal tumors predict clinical outcome. *Science* 313: 1960-1964, 2006.
6. Galon J, Fridman WH and Pagès F: The adaptive immunologic microenvironment in colorectal cancer: A novel perspective. *Cancer Res* 67: 1883-1886, 2007.
7. Marabelle A, Fakih M, Lopez J, Shah M, Shapira-Frommer R, Nakagawa K, Chung HC, Kindler HL, Lopez-Martin JA, Miller WH Jr, *et al*: Association of tumour mutational burden with outcomes in patients with advanced solid tumours treated with pembrolizumab: Prospective biomarker analysis of the multicohort, open-label, phase 2 KEYNOTE-158 study. *Lancet Oncol* 21: 1353-1365, 2020.
8. Galon J, Mlecnik B, Bindea G, Angell HK, Berger A, Lagorce C, Lugli A, Zlobec I, Hartmann A, Bifulco C, *et al*: Towards the introduction of the 'Immunoscore' in the classification of malignant tumours. *J Pathol* 232: 199-209, 2014.
9. Schumacher TN and Schreiber RD: Neoantigens in cancer immunotherapy. *Science* 348: 69-74, 2015.
10. Galon J and Bruni D: Tumor immunology and tumor evolution: Intertwined histories. *Immunity* 52: 55-81, 2020.
11. Weiser MR: AJCC 8th edition: Colorectal cancer. *Ann Surg Oncol* 25: 1454-1455, 2018.
12. Yomoda T, Sudo T, Kawahara A, Shigaki T, Shimomura S, Tajiri K, Nagasu S, Fujita F, Kinugasa T and Akagi Y: The immunoscore is a superior prognostic tool in stages II and III colorectal cancer and is significantly correlated with programmed death-ligand 1 (PD-L1) expression on tumor-infiltrating mononuclear cells. *Ann Surg Oncol* 26: 415-424, 2019.
13. Schneider CA, Rasband WS and Eliceiri KW: NIH image to ImageJ: 25 years of image analysis. *Nat Methods* 9: 671-675, 2012.
14. Fujiyoshi K, Bruford EA, Mroz P, Sims CL, O'Leary TJ, Lo AWI, Chen N, Patel NR, Patel KP, Seliger B, *et al*: Opinion: Standardizing gene product nomenclature-a call to action. *Proc Natl Acad Sci USA* 118: e2025207118, 2021.
15. Kirilovsky A, Marliot F, El Sissy C, Haicheur N, Galon J and Pagès F: Rational bases for the use of the immunoscore in routine clinical settings as a prognostic and predictive biomarker in cancer patients. *Int Immunol* 28: 373-382, 2016.

16. Chaudhary R, Quagliata L, Martin JP, Alborelli I, Cyanam D, Mittal V, Tom W, Au-Young J, Sadis S and Hyland F: A scalable solution for tumor mutational burden from formalin-fixed, paraffin-embedded samples using the oncomine tumor mutation load assay. *Transl Lung Cancer Res* 7: 616-630, 2018.
17. Hellmann MD, Ciuleanu TE, Pluzanski A, Lee JS, Otterson GA, Audigier-Valette C, Minenza E, Linardou H, Burgers S, Salman P, *et al*: Nivolumab plus ipilimumab in lung cancer with a high tumor mutational burden. *N Engl J Med* 378: 2093-2104, 2018.
18. Overman MJ, Lonardi S, Wong KYM, Lenz HJ, Gelsomino F, Aglietta M, Morse MA, Van Cutsem E, McDermott R, Hill A, *et al*: Durable clinical benefit with nivolumab plus ipilimumab in DNA mismatch repair-deficient/microsatellite instability-high metastatic colorectal cancer. *J Clin Oncol* 36: 773-779, 2018.
19. Noepel-Duennebacke S, Juette H, Schulmann K, Graeven U, Porschen R, Stoecklacher J, Hegewisch-Becker S, Raulf A, Arnold D, Reinacher-Schick A and Tannapfel A: Microsatellite instability (MSI-H) is associated with a high immunoscore but not with PD-L1 expression or increased survival in patients (pts.) with metastatic colorectal cancer (mCRC) treated with oxaliplatin (ox) and fluoropyrimidine (FP) with and without bevacizumab (bev): A pooled analysis of the AIO KRK 0207 and RO91 trials. *J Cancer Res Clin Oncol* 147: 3063-3072, 2021.
20. de Jong AE, van Puijenbroek M, Hendriks Y, Tops C, Wijnen J, Ausems MG, Meijers-Heijboer H, Wagner A, van Os TA, Bröcker-Vriends AH, *et al*: Microsatellite instability, immunohistochemistry, and additional PMS2 staining in suspected hereditary nonpolyposis colorectal cancer. *Clin Cancer Res* 10: 972-980, 2004.
21. Truninger K, Menigatti M, Luz J, Russell A, Haider R, Gebbers JO, Bannwart F, Yurtsever H, Neuweiler J, Riehle HM, *et al*: Immunohistochemical analysis reveals high frequency of PMS2 defects in colorectal cancer. *Gastroenterology* 128: 1160-1171, 2005.
22. Senter L, Clendenning M, Sotamaa K, Hampel H, Green J, Potter JD, Lindblom A, Lagerstedt K, Thibodeau SN, Lindor NM, *et al*: The clinical phenotype of Lynch syndrome due to germ-line PMS2 mutations. *Gastroenterology* 135: 419-428, 2008.
23. Ten Broeke SW, van der Klift HM, Tops CMJ, Aretz S, Bernstein I, Buchanan DD, de la Chapelle A, Capella G, Clendenning M, Engel C, *et al*: Cancer risks for PMS2-associated Lynch syndrome. *J Clin Oncol* 36: 2961-2968, 2018.
24. Chan TA, Yarchoan M, Jaffee E, Swanton C, Quezada SA, Stenzinger A and Peters S: Development of tumor mutation burden as an immunotherapy biomarker: Utility for the oncology clinic. *Ann Oncol* 30: 44-56, 2019.
25. Hwang HS, Kim D and Choi J: Distinct mutational profile and immune microenvironment in microsatellite-unstable and POLE-mutated tumors. *J Immunother Cancer* 9: e002797, 2021.
26. Salem ME, Bodor JN, Puccini A, Xiu J, Goldberg RM, Grothey A, Korn WM, Shields AF, Worilow WM, Kim ES, *et al*: Relationship between MLH1, PMS2, MSH2 and MSH6 gene-specific alterations and tumor mutational burden in 1057 microsatellite instability-high solid tumors. *Int J Cancer* 147: 2948-2956, 2020.
27. Boland CR and Goel A: Microsatellite instability in colorectal cancer. *Gastroenterology* 138: 2073-2087.e3, 2010.
28. Le DT, Durham JN, Smith KN, Wang H, Bartlett BR, Aulakh LK, Lu S, Kemberling H, Wilt C, Luber BS, *et al*: Mismatch repair deficiency predicts response of solid tumors to PD-1 blockade. *Science* 357: 409-413, 2017.
29. Angelova M, Charoentong P, Hackl H, Fischer ML, Snajder R, Krogsdam AM, Waldner MJ, Bindea G, Mlecnik B, Galon J and Trajanoski Z: Characterization of the immunophenotypes and antigenomes of colorectal cancers reveals distinct tumor escape mechanisms and novel targets for immunotherapy. *Genome Biol* 16: 64, 2015.
30. Giannakis M, Mu XJ, Shukla SA, Qian ZR, Cohen O, Nishihara R, Bahl S, Cao Y, Amin-Mansour A, Yamauchi M, *et al*: Genomic correlates of immune-cell infiltrates in colorectal carcinoma. *Cell Rep* 15: 857-865, 2016.
31. Pagès F, Mlecnik B, Marliot F, Bindea G, Ou FS, Bifulco C, Lugli A, Zlobec I, Rau TT, Berger MD, *et al*: International validation of the consensus Immunoscore for the classification of colon cancer: A prognostic and accuracy study. *Lancet* 391: 2128-2139, 2018.
32. Mlecnik B, Bindea G, Angell HK, Maby P, Angelova M, Tougeron D, Church SE, Lafontaine L, Fischer M, Fredriksen T, *et al*: Integrative analyses of colorectal cancer show immunoscore is a stronger predictor of patient survival than microsatellite instability. *Immunity* 44: 698-711, 2016.
33. Chalabi M, Fanchi LF, Dijkstra KK, Van den Berg JG, Aalbers AG, Sikorska K, Lopez-Yurda M, Grootsholten C, Beets GL, Snaebjornsson P, *et al*: Neoadjuvant immunotherapy leads to pathological responses in MMR-proficient and MMR-deficient early-stage colon cancers. *Nat Med* 26: 566-576, 2020.
34. Chakrabarti S, Huebner LJ, Finnes HD, Muranyi A, Singh S, Clements J, McWilliams RR, Hubbard JM, Shanmugam K and Sinicrope FA: Intratumoral CD3⁺ and CD8⁺ T-cell densities in patients with deficient DNA mismatch repair (dMMR) metastatic colorectal cancer (mCRC) receiving programmed death-1 (PD-1) blockade. *J Clin Oncol* 37 (15 Suppl): S3532, 2019.
35. Chatterjee N and Walker GC: Mechanisms of DNA damage, repair, and mutagenesis. *Environ Mol Mutagen* 58: 235-263, 2017.
36. Nicolas E, Golemis EA and Arora S: POLD1: Central mediator of DNA replication and repair, and implication in cancer and other pathologies. *Gene* 590: 128-141, 2016.
37. Fabrizio DA, George TJ Jr, Dunne RF, Frampton G, Sun J, Gowen K, Kennedy M, Greenbowe J, Schrock AB, Hezel AF, *et al*: Beyond microsatellite testing: Assessment of tumor mutational burden identifies subsets of colorectal cancer who may respond to immune checkpoint inhibition. *J Gastrointest Oncol* 9: 610-617, 2018.
38. Santin AD, Bellone S, Buza N, Choi J, Schwartz PE, Schlessinger J and Lifton RP: Regression of chemotherapy-resistant polymerase ϵ (POLE) ultra-mutated and MSH6 hyper-mutated endometrial tumors with nivolumab. *Clin Cancer Res* 22: 5682-5687, 2016.
39. Monu NR and Frey AB: Myeloid-derived suppressor cells and anti-tumor T cells: A complex relationship. *Immunol Invest* 41: 595-613, 2012.
40. Samstein RM, Lee CH, Shoushtari AN, Hellmann MD, Shen R, Janjigian YY, Barron DA, Zehir A, Jordan EJ, Omuro A, *et al*: Tumor mutational load predicts survival after immunotherapy across multiple cancer types. *Nat Genet* 51: 202-206, 2019.
41. Marabelle A, Fakih MG, Lopez J, Shah M, Shapira-Frommer R, Nakagawa K, Chung HC, Kindler HL, Lopez-Martin JA, Miller W, *et al*: 1192O-Association of tumor mutational burden with outcomes in patients with select advanced solid tumors treated with pembrolizumab in KEYNOTE-158. *Ann Oncol* 30: v477-v478, 2019.



This work is licensed under a Creative Commons Attribution-NonCommercial-NoDerivatives 4.0 International (CC BY-NC-ND 4.0) License.